Theoretical Investigation of the Design of Aluminum Gallium Nitride Cathodes

C.W. Hatfield and G.L. Bilbro
Department of Electrical and Computer Engineering
North Carolina State University
Raleigh, NC 27695
cwhatfie@eos.ncsu.edu, glb@eos.ncsu.edu

Abstract

The goal of this work was to theoretically investigate how the room temperature (300 K) performance of an aluminum gallium nitride ($Al_xGa_{1-x}N$) cathode would vary with variations in thickness, doping, and compositional grading.

1 Introduction

Semiconductor materials which exhibit low, zero, or negative electron affinity have been extensively researched for their use as cathodes. Among these materials are various forms of carbon (particularly diamond) and III-V nitride materials such as boron nitride (BN) and aluminum gallium nitride ($Al_xGa_{1-x}N$). However, the fabrication of a useful cathode from one of these materials imposes certain requirements. These requirements appear to be satisfied by $Al_xGa_{1-x}N$. These requirements include the ability to grow a high-quality film upon an available substrate [1,2], the ability to perform n-type doping [3,4], and the formation of an ohmic contact somewhere on the cathode structure [5,6].

The observation of negative electron affinity (NEA) for heteroepitaxial AlN by way of ultraviolet photoemission spectroscopy (UPS) originally inspired the idea of using layers of $Al_xGa_{1-x}N$ as a NEA cold cathode [7]. Currently, a controversy exists with respect to the electron affinity of various III-V nitride materials. A group at North Carolina State University continues to maintain that AlN has a *negative* electron affinity [8,9]. A group at the Naval Research Laboratory believes that AlN has a small positive electron affinity, on the order of 0.6 eV [10]. Other groups, based at Princeton University and at Lucent Technologies, has reported that AlN has a positive electron affinity on the order of 2 eV [11]. However, it appears that the experimental data obtained by these three groups is very similar, but the manner in which the data is interpreted is ambiguous, leading to uncertainty about the *true* value of the electron affinity. For these cathode simulations, we are interested specifically in electron affinity data for $Al_xGa_{1-x}N$ material for which the value of x is equal to or less than 0.75. Such data has been collected by Nemanich *et al.* at North Carolina

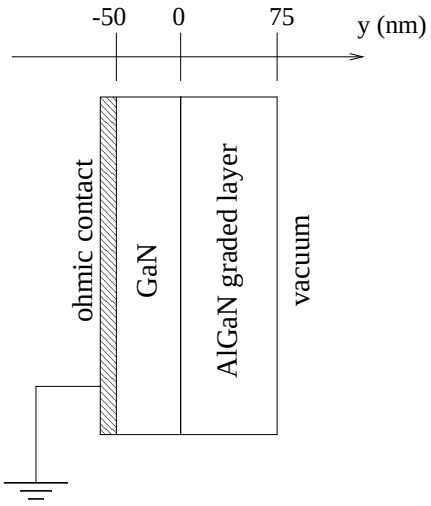

Figure 1: Basic cathode structure.

State University, and it has been published [8,9]. We use *this* data as the basis for our simulations.

Graded electron affinity cold cathodes made from $Al_xGa_{1-x}N$ material have been described, Poisson's equation has been solved, and the maximum current density has been estimated for undoped $Al_xGa_{1-x}N$ structures [12]. $Al_xGa_{1-x}N$ cathodes with a compositionally-graded layer (x from 0.0 to 0.9) upon an n-type GaN layer have been fabricated, and electron emission measurements have been done using an extraction grid structure [13,14].

In our previous work [15], we presented simulations of a cathode with an n-type, graded layer of $Al_xGa_{1-x}N$ on n-type GaN. These simulations described the expected emission of a basic cathode structure at room temperature both with zero applied electric field (thermal equilibrium) and also in cases in which an external electric field is applied to the cathode surface. In this new work, we examine the ramifications of changing the cathode's layer thicknesses, n-type doping level, and compositional grading profile.

2 Methodology

The basic cathode structure is shown in Figure 1. The cathode structure has a linear grading of Al fraction (x) with position (y) in which the value of x rises from x=0.00 to x=0.75 over a distance of 75 nm. The coordinate system is defined such that the origin $y = 0$ is located at the interface between the GaN layer and the graded layer. It is assumed for the purpose of the simulation that the linearly graded layer is grown upon a 50-nm-thick layer of GaN. The GaN layer has an ohmic contact on the back, and the ohmic contact is connected to ground. Consequently, the location of the vacuum level at the back of the cathode (y=-50 nm) is used as the zero energy reference.

Reports on the n-type doping of GaN and AlGaN with Si indicate dopant concentrations

in the range of 10^{17} to 10^{19} cm^{-3} [3,4]. The incorporation of higher concentrations of Si tends to cause cracking in the films [16]. For the purpose of these calculations, the cathode is assumed to be doped uniformly with Si at a concentration of 10^{18} cm^{-3} throughout the entire cathode structure. The concentration 10^{18} cm^{-3} is a relatively high concentration, with respect to film growth considerations; however, as shown in the subsequent calculations, it provides a low emission barrier.

The effective mass of an electron in $Al_xGa_{1-x}N$ was assumed to be that of GaN ($0.19m_o$) for all values of x [17]. The results of quantum molecular dynamics calculations performed by Boguslawski and Bernholc [18] were combined with experimental Hall effect data taken by Bremser, *et al.* [4] from Si-doped $Al_xGa_{1-x}N$ films to specify the ionization energy of Si in $Al_xGa_{1-x}N$ as a function of Al fraction x. The mathematical function $E_{CD} = 0.030 + 0.627x$ (eV) describes the Si atom ionization energies used for these calculations.

A conduction band offset between AlN and GaN of 1.92 eV was calculated by Majewski and Staedele [19] using a first-principles total-energy pseudopotential method. That is, when grown adjacent to each other, the conduction band minimum energies of AlN and GaN are separated by 1.92 eV. Therefore, assuming that a simple linear function describes the offset as a function of x, then the offset between GaN and $Al_{0.75}Ga_{0.25}N$ should be 0.75×1.92 eV = 1.44 eV. That is, if GaN and $Al_{0.75}Ga_{0.25}N$ are grown adjacent to each other, their minimum conduction band energies will be separated by 1.44 eV. This heterojunction conduction band offset was taken into account in this simulation by defining a local vacuum level inside the cathode structure at each point and describing the energy separation between the local vacuum level and the conduction band minimum energy using a function of Al fraction x which is 1.44 - 1.92x eV.

To compute the energy barrier seen by electrons attempting to escape to vacuum, Poisson's equation [20]

$$\frac{\partial^2 \varphi}{\partial y^2} = -\frac{\rho}{\epsilon_s} - \frac{1}{\epsilon_s}\frac{\partial \varphi}{\partial y}\frac{\partial \epsilon_s}{\partial y} \tag{1}$$

must be solved, where φ is potential, y is position, ρ is charge density (consisting of free electrons and ionized donor atoms), and ϵ_s is the semiconductor permittivity. (Note that relative permittivity has been reported [21] for GaN and AlN to be 9.0 and 8.5, respectively. Consequently, an average value of 8.75 was used in the simulation for all values of x, in order to simplify Poisson's equation and eliminate the second term on the right hand side.) The equation was solved by implementing a Runge-Kutta numerical procedure [22] on *Maple V* mathematical software [23].

The conduction band minimum energy corresponding to the potential distribution is $E_C = -q\varphi - \Delta E_C$, where ΔE_C is the heterojunction conduction band offset. Physically, the heterojunction conduction band offset is defined as the energy difference between the local vacuum level and the conduction band minimum energy. The position of the local vacuum energy level is determined by the potential.

Based on the thermionic emission theory of metal-semiconductor junctions, the expected

emitted current density is [24]

$$J = A^* T^2 \exp(\frac{-q\phi}{kT}) \tag{2}$$

where J is current density, A^* is the Richardson constant, T is temperature, k is Boltzmann's constant, and ϕ is the barrier height. The Richardson constant is given by [24]

$$A^* = \frac{4\pi q m^* k^2}{h^3} \tag{3}$$

where h is Planck's constant and m^* is the effective mass of electrons. The barrier for electrons attempting to escape out to vacuum is given by the energy difference between the minimum conduction band energy and the Fermi level energy at the cathode-vacuum interface, i.e. $q\phi = E_C$ - E_F at $y = 75$ nm.

As is the case for metal-semiconductor junctions, the current transport can be limited by both the energy barrier and electron diffusion. The diffusion current density at the cathode-vacuum interface is [24]

$$J_D = qD_n \frac{\partial n}{\partial y} = \mu_n kT \frac{\partial n}{\partial y} \tag{4}$$

where J_D is the diffusion current density, D_n is the electron diffusivity, n is the free electron concentration, and μ_n is the electron mobility. The electron concentration as a function of position is computed from the conduction band and the Fermi level.

Experimental data for electron mobility in $Al_xGa_{1-x}N$ which is heavily doped in the range of 4.5×10^{18} to 1.2×10^{20} exists. This data was reported in 1998 [4], and is plotted in Figure 2. The authors are not aware of data for material for which $x > 0.58$, but it could be roughly ascertained from the data that an electron mobility of about 30 cm^2/V-s for $x = 0.75$ material would not be unreasonable. This value of electron mobility is used later for diffusion current calculations.

3 Results

3.1 Basic Cathode Structure Operation at 300 K

The most basic $Al_xGa_{1-x}N$ cathode design assumed in this work is a structure of the form shown in Figure 1, in which an $Al_xGa_{1-x}N$ layer sits upon a GaN layer. The $Al_xGa_{1-x}N$ layer is compositionally graded from $x = 0.00$ to $x = 0.75$ over a thickness of 75 nm. The grading is linear with position, i.e. Al fraction x varies with y as $10^7 y$, where y is the position in meters. The cathode structure is doped uniformly n-type with Si at a concentration of 10^{18} cm^{-3}. At 300 K, the Fermi level in the GaN material with 10^{18} cm^{-3} Si doping is located 0.041 eV below the conduction band.

The conduction band minimum energy and Fermi level as a function of position in the basic cathode structure is shown in Figure 3. The energy values are referenced to the back of

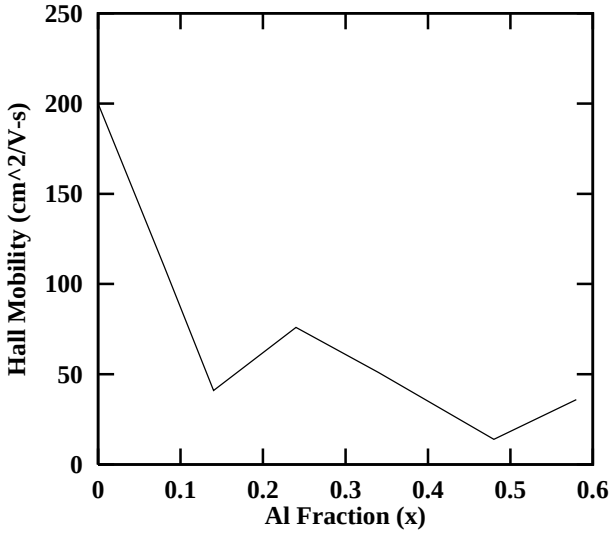

Figure 2: Electron mobility vs. Al fraction (x) for $Al_xGa_{1-x}N$ material.

the GaN layer, at which an ohmic contact is grounded. This ground is taken as both the zero energy and zero potential references. The conduction band minimum energy at the back of the GaN layer starts at -1.44 eV, which corresponds to the heterojunction conduction band offset of the GaN material. The band dips down to about -1.46 eV at the origin. It rises up to -0.92 eV at the cathode-vacuum interface, corresponding to the value of potential there.

The Fermi level (E_F) is located at -1.481 eV, as shown in Figure 3. The energy barrier for electrons attempting to escape into vacuum is the energy difference between the conduction band minimum energy and the Fermi level at the cathode-vacuum interface, and this value is 0.560 eV. At 300 K, thermionic emission theory indicates an emission density of 7.92 A/m^2, or 792 μA/cm^2.

The concentration of electrons at the back of the the GaN layer is 4.31×10^{17} cm^{-3}. The electron concentration rises up to about 1.4×10^{18} cm^{-3} at the origin and then rapidly drops off into the $Al_xGa_{1-x}N$ layer. This electron distribution results in a diffusion current at the cathode-vacuum interface that supplies electrons during emission. The gradient of electron concentration at the interface is 8.90×10^{15} cm^{-4}. With this gradient, the electron mobility required at the cathode-vacuum interface to achieve the emission density indicated by thermionic emission theory is 21.3 cm^2/V-s. Based on the mobility data for $Al_xGa_{1-x}N$ materials indicating that $\mu_n \approx 30$ cm^2/V-s for the $x = 0.75$ material, the current will probably be barrier-limited, not diffusion-limited.

3.2 Cathodes with a Thicker $Al_xGa_{1-x}N$ Layer

$Al_xGa_{1-x}N$ graded layers can be grown with varying thicknesses. The effect of making the layer thicker was studied by simulating cathodes with graded layers with linear grading which were 0.25 μm thick and 0.50 μm thick.

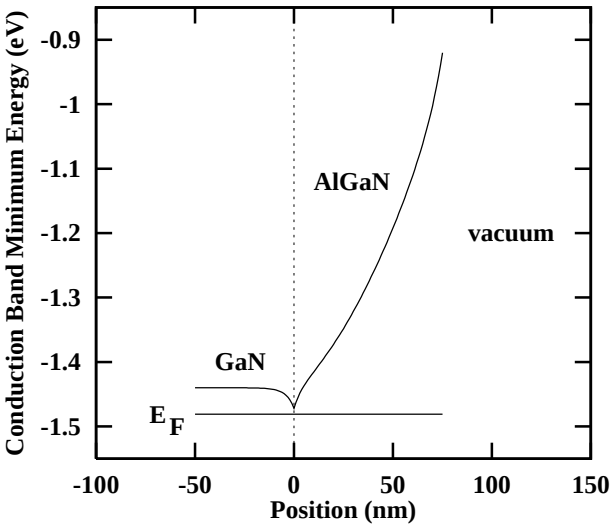

Figure 3: Conduction band minimum energy vs. position in basic cathode structure at 300 K.

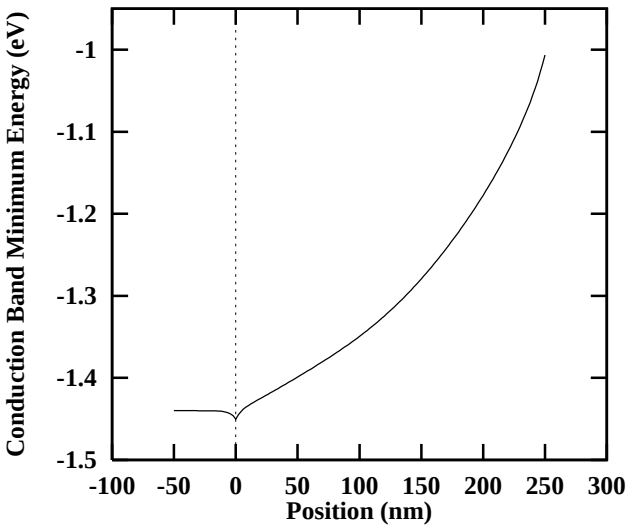

Figure 4: Conduction band minimum energy vs. position for a cathode with 0.25-μm-thick $Al_xGa_{1-x}N$ layer.

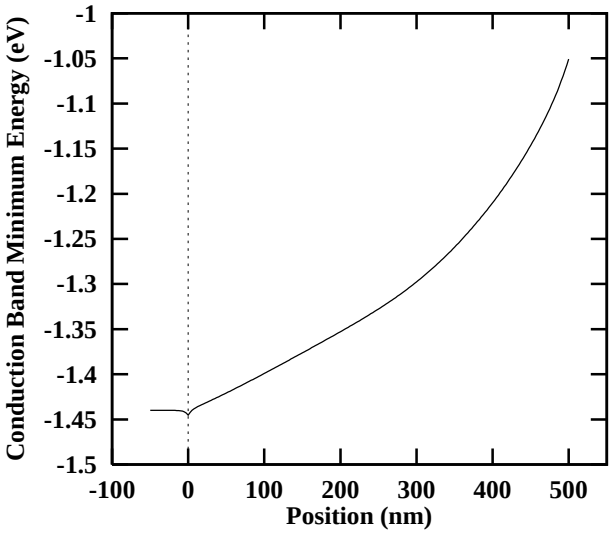

Figure 5: Conduction band minimum energy vs. position for a cathode with a 0.50-μm-thick $Al_xGa_{1-x}N$ layer.

3.2.1 Cathode with 0.25-μm-Thick $Al_xGa_{1-x}N$ Layer

The conduction band minimum energy as a function of position for a cathode structure with a 0.25-μm-thick $Al_xGa_{1-x}N$ layer is shown in Figure 4. The 0.25-μm-thick layer is graded linearly with position, i.e. the Al fraction varies as $3 \times 10^6 y$, where y is given in meters.

The conduction band rises up to -1.006 eV at the cathode-vacuum interface. The Fermi level is located at -1.481 eV. The energy barrier for electrons attempting to escape into vacuum is 0.474 eV, down from 0.560 eV observed with the 75-nm-thick $Al_xGa_{1-x}N$ layer. At 300 K, thermionic emission theory indicates an emission density of 221 A/m^2, or 22.1 mA/cm^2, which is much higher than the 792 μA/cm^2 predicted for the 75-nm-thick $Al_xGa_{1-x}N$ layer.

The gradient of electron concentration at the cathode-vacuum interface in this case is 6.31×10^{16} cm^{-4}. With this gradient, the electron mobility required at the cathode-vacuum interface to achieve the emission density indicated by thermionic emission theory is 84.6 cm^2/V-s. Based on the mobility data for $Al_xGa_{1-x}N$ layers indicating that $\mu_n \approx 30$ cm^2/V-s for the $x = 0.75$ material, the current density for this structure will probably be diffusion-limited, not barrier-limited. The expected value of emission current density based on this lower mobility value would be 7.8 mA/cm^2.

3.2.2 Cathode with 0.50-μm-thick $Al_xGa_{1-x}N$ Layer

The conduction band minimum energy as a function of position for a cathode structure with a 0.50-μm-thick $Al_xGa_{1-x}N$ layer is shown in Figure 5. The 0.50-μm-thick layer is graded linearly with position, i.e. the Al fraction varies as $1.5 \times 10^6 y$, where y is given in meters.

The conduction band rises up to -1.051 eV at the cathode-vacuum interface. The Fermi level is located at -1.481 eV. The energy barrier for electrons attempting to escape into vac-

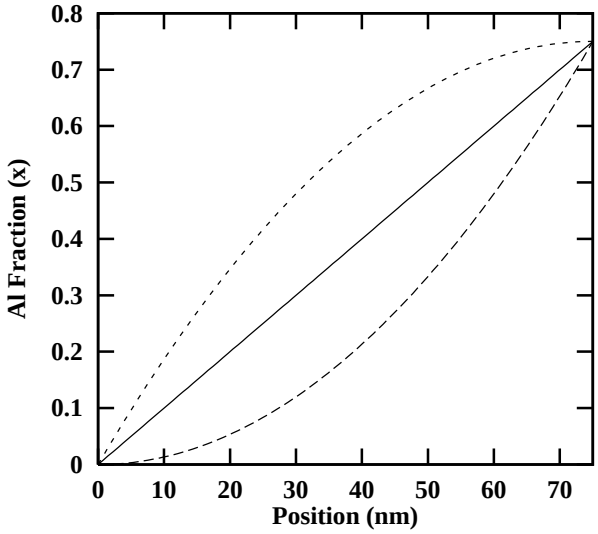

Figure 6: Linear and quadratic grading profiles for the $Al_xGa_{1-x}N$ layer.

uum is 0.430 eV, down from 0.560 eV observed with the 75-nm-thick $Al_xGa_{1-x}N$ layer. At 300 K, thermionic emission theory indicates an emission density of 1221 A/m^2, or 0.1221 mA/cm^2, which is much higher than the 792 μA/cm^2 predicted for the 75-nm-thick $Al_xGa_{1-x}N$ layer.

The gradient of electron concentration at the cathode-vacuum interface in this case is 1.46×10^{17} cm^{-4}. With this gradient, the electron mobility required at the cathode-vacuum interface to achieve the emission density indicated by thermionic emission theory is 201.8 cm^2/V-s. Based on the mobility data for $Al_xGa_{1-x}N$ layers indicating that $\mu_n \approx 30$ cm^2/V-s for the $x = 0.75$ material, the current density for this structure will definitely be diffusion-limited, not barrier-limited. The expected value of emission current density, based on this lower mobility value, would be 18.1 mA/cm^2.

3.3 Cathodes with Non-Linear Grading

To investigate the effect of using various types of grading profiles, two non-linear grading profiles in the $Al_xGa_{1-x}N$ layer were studied. The first profile was a quadratic function which had $x = 0.00$ at the GaN-$Al_xGa_{1-x}N$ interface, $x = 0.75$ at the cathode-vacuum interface, and was concave up, i.e., $1.333 \times 10^{14} y^2$ where y is given in meters. The second profile was a quadratic function which had $x = 0.00$ at the GaN-$Al_xGa_{1-x}N$ interface, $x = 0.75$ at the cathode-vacuum interface, and was concave down, i.e., $-1.333 \times 10^{14} y^2 + 2 \times 10^7 y$ where y is given in meters. These two non-linear profiles, along with the basic linear profile, are plotted in Figure 6.

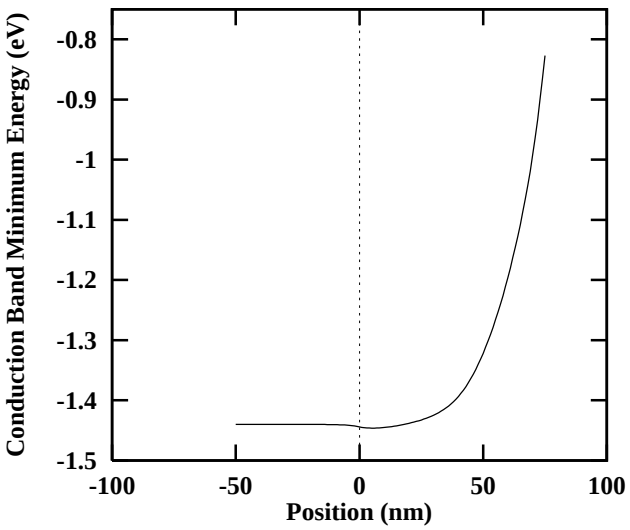

Figure 7: Conduction band minimum energy vs. position for a basic cathode structure with a concave-up quadratic grading.

3.3.1 Cathode with Concave-Up Quadratic Grading

The conduction band minimum energy as a function of position for a cathode structure with the concave-up quadratic grading profile in the $Al_xGa_{1-x}N$ layer is shown in Figure 7. The shape of the conduction band curve is quite different for this grading than the linear grading case (see Figure 3). There is no sharp downward dip at the origin, and the curve rises with upward concavity to -0.827 eV.

The Fermi level is located at -1.481 eV. The energy barrier for electrons attempting to escape into vacuum is 0.654 eV, up from 0.560 eV observed with the linear grading. At 300 K, thermionic emission theory indicates an emission density of 0.2137 A/m^2, or 21.37 μA/cm^2, which is lower than the 792 μA/cm^2 predicted for the linear grading.

The gradient of electron concentration at the cathode-vacuum interface in this case is 7.40×10^{14} cm^{-4}. With this gradient, the electron mobility required at the cathode-vacuum interface to achieve the emission density indicated by thermionic emission theory is 6.98 cm^2/V-s. For this structure, based on the $Al_xGa_{1-x}N$ mobility data indicating that $\mu_n \approx$ 30 cm^2/V-s for the $x = 0.75$ material, the current is most likely barrier-limited, rather than diffusion-limited.

3.3.2 Cathode with Concave-Down Quadratic Grading

The conduction band minimum energy as a function of position for a cathode structure with the concave-down quadratic grading profile in the $Al_xGa_{1-x}N$ layer is shown in Figure 8. The shape of the conduction band curve is quite different for this grading than the linear grading case (see Figure 3). The dip at the origin is more pronounced, and the curve rises up with downward concavity to -1.003 eV.

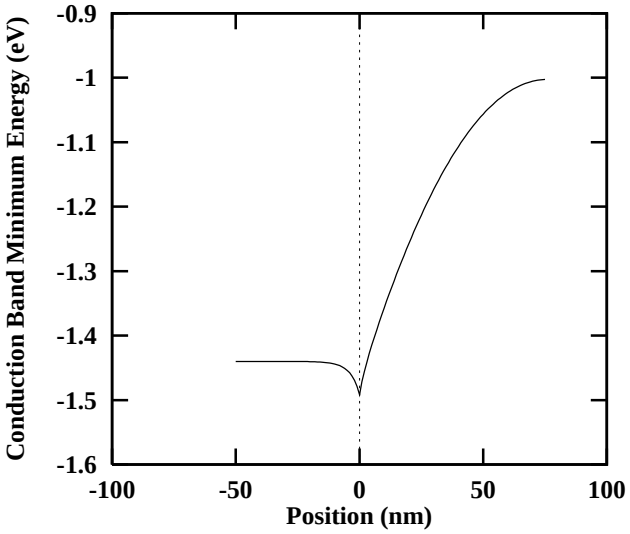

Figure 8: Conduction band minimum energy vs. position for a cathode with a concave-down quadratic grading.

The Fermi level is located at -1.481 eV. The energy barrier for electrons attempting to escape into vacuum is 0.478 eV, down from 0.560 eV observed with the linear grading. At 300 K, thermionic emission theory indicates an emission density of 191.4 A/m^2, or 19.14 mA/cm^2, which is higher than the 792 μA/cm^2 predicted for the linear grading.

The gradient of electron concentration at the cathode-vacuum interface in this case is 1.89×10^{15} cm^{-4}. With this gradient, the electron mobility required at the cathode-vacuum interface to achieve the emission density indicated by thermionic emission theory is 2444 cm^2/V-s. For this structure, based on the $Al_xGa_{1-x}N$ mobility data indicating that $\mu_n \approx$ 30 cm^2/V-s for the $x = 0.75$ material, the current will definitely be diffusion-limited. The expected value of emission current density, based on this lower mobility value, would be 235 μA/cm^2.

3.4 Cathodes with Moderate and Low Donor Concentrations

The baseline cathode simulations were performed for structures in which the donor concentration was 1×10^{18} cm^{-3} (a "high" concentration). To create a substantial free electron concentration, the donor concentration should be kept high. However, as mentioned previously, $Al_xGa_{1-x}N$ film growth studies indicate that excess Si impurities in such films lead to cracking. Therefore, it is important to study the emission properties of cathode structures with varying donor concentrations. Cathode structures containing 5×10^{17} cm^{-3} (a "moderate" concentration) and 1×10^{17} cm^{-3} (a "low" concentration) were also simulated. Note that, in order to perform these simulations, the position of the Fermi level in the n-GaN layer had to be recalculated each time.

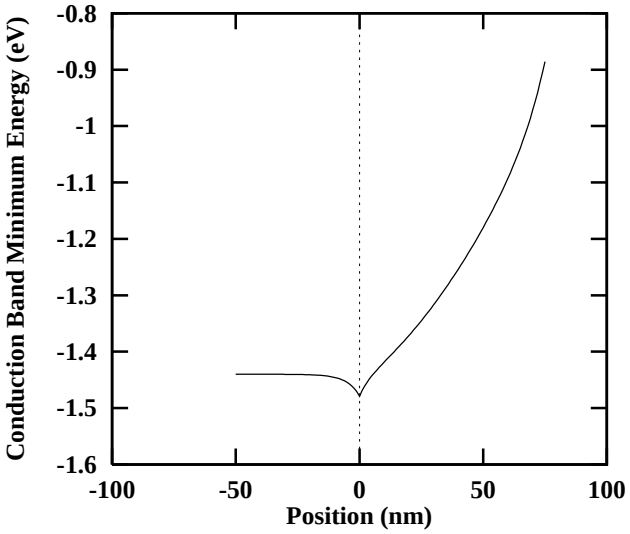

Figure 9: Conduction band minimum energy vs. position for a basic cathode structure with a moderate donor concentration of 5×10^{17} cm^{-3}.

3.4.1 Cathode Structure with Moderate Donor Concentration

The conduction band minimum energy as a function of position for a cathode structure with moderate donor concentration (5×10^{17} cm^{-3}) is shown in Figure 9. The conduction band rises up with upward concavity to -0.886 eV. The Fermi level is located at -1.493 eV. The energy barrier for electrons attempting to escape into vacuum is 0.607 eV, up from 0.560 eV observed with the higher donor concentration. At 300 K, thermionic emission theory indicates an emission density of 1.315 A/m^2, or 131.5 μA/cm^2, which is lower than the 792 μA/cm^2 predicted for the high donor concentration.

The gradient of electron concentration at the cathode-vacuum interface in this case is 1.481×10^{15} cm^{-4}. With this gradient, the electron mobility required at the cathode-vacuum interface to achieve the emission density indicated by thermionic emission theory is 21.47 cm^2/V-s. For this structure, based on the $Al_xGa_{1-x}N$ mobility data indicating that $\mu_n \approx 30$ cm^2/V-s for the $x = 0.75$ material, the current density will probably be barrier-limited, not diffusion-limited.

3.4.2 Cathode Structure with Low Donor Concentration

The conduction band minimum energy as a function of position for a cathode structure with a low donor concentration (1×10^{17} cm^{-3}) is shown in Figure 10. The conduction band rises with upward concavity to -0.588 eV. The Fermi level is located at -1.524 eV. The energy barrier for electrons attempting to escape into vacuum is 0.936 eV, which is much larger than the 0.560 eV observed with the high concentration. At 300 K, thermionic emission theory indicates an emission density of 3.89×10^{-6} A/m^2, or 389 pA/cm^2, which is much lower than the 792 μA/cm^2 predicted for the high concentration. Clearly, reducing the donor

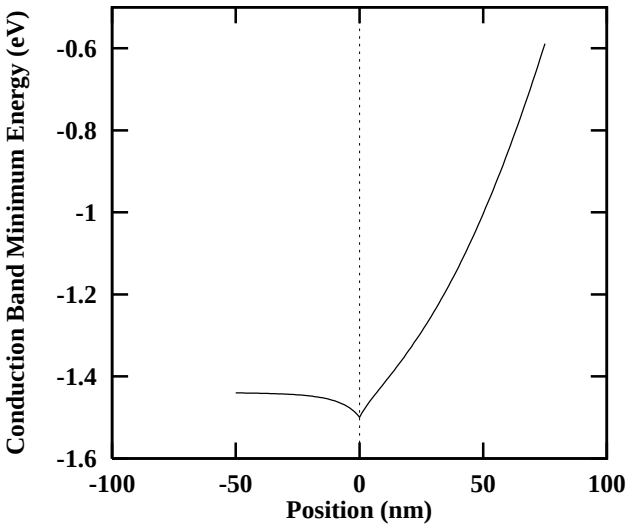

Figure 10: Conduction band minimum energy vs. position for a basic cathode structure with a low donor concentration of 1×10^{17} cm^{-3}.

concentration to this level makes the emission barrier unacceptably high, comparable to that observed for conventional thermionic cathodes.

The gradient of electron concentration at the cathode-vacuum interface in this case is 4.35×10^{9} cm^{-4}. With this gradient, the electron mobility required at the cathode-vacuum interface to achieve the emission density indicated by thermionic emission theory is 21.66 cm^2/V-s. For this structure, based on the $Al_xGa_{1-x}N$ mobility data indicating that $\mu_n \approx$ 30 cm^2/V-s for the $x = 0.75$ material, the current would probably be barrier-limited, not diffusion-limited.

4 Conclusions

A summary of the results for the cathode simulations performed in this study are shown in Table 6.1. The current values refer to the amount of current which would be emitted by a 1 cm^2 cathode. The diffusion-limited current density of cathode structures which have a current density limited by difusion were computed by assuming that the electron mobility in the $x = 0.75$ material is 30 cm^2/V-s. "B-L Curr." refers to barrier-limited current, "D-L Curr." refers to diffusion-limited current, and "Exp. Curr." refers to the current which would be expected when both barrier- and diffusion-limiting are taken into account. These results for $Al_xGa_{1-x}N$ cathode structures lead to many important guidelines concerning the design and operation of $Al_xGa_{1-x}N$ cathodes.

The use of n-type doping and compositional grading appears to be an effective means of creating an $Al_xGa_{1-x}N$ cathode with a very low thermionic emission barrier. The superpositioning of the n-type doping with the grading results in a charge distribution which brings

Structure	Barrier	B-L Curr.	D-L Curr.	Exp. Curr.
basic (300 K)	0.560 eV	792 μA	1.13 mA	792 μA
0.25 μm (300 K)	0.474 eV	22.1 mA	7.8 mA	7.8 mA
0.50 μm (300 K)	0.430 eV	122 mA	18.1 mA	18.1 mA
concave up (300 K)	0.654 eV	21.4 μA	91.7 μA	21.4 μA
concave down (300 K)	0.478 eV	19.1 mA	235 μA	235 μA
moderate N_D (300 K)	0.607 eV	132 μA	189 μA	132 μA
low N_D (300 K)	0.936 eV	389 pA	530 μA	389 pA

Table 1: Summary of Cathode Simulation Results

the conduction band at the surface down towards the Fermi level, resulting in a very low thermionic emission barrier.

The basic cathode structure, which utilized a 75-nm-thick $Al_xGa_{1-x}N$ layer with its Al fraction (x) varied linearly with position and a constant doping of $10^{18}cm^{-3}$, exhibited a barrier of just 0.560 eV at 300 K. This emission barrier is much lower than that generally observed for commercially available thermionic cathodes (1 eV or more) [25].

Simulations were performed for $Al_xGa_{1-x}N$ layers of thickness 0.25 μm and 0.50 μm. These simulations clearly indicate that increasing the thickness of the $Al_xGa_{1-x}N$ layer substantially reduces the emission barrier. The emission from these thicker structures is diffusion-limited, but the emitted current density at 300 K is more than an order of magnitude larger than that of the 0.075-μm-thick structure. Hence, increasing the layer thickness is a useful technique for increasing current density. Unfortunately, there is a limit to how thick the $Al_xGa_{1-x}N$ layer can be, based on film growth considerations.

Simulations done for Si doping levels below $10^{18}cm^{-3}$ indicate that the emission barrier is a strong function of doping. Reducing the doping by a factor of 2 increased the barrier by about 8%, which lowers the room temperature current density to 17% of its original value. Reducing the doping by a factor of 10 increased the barrier by more than 67%, which decreases the room temperature emission by a factor of more than 10^6. Obviously, excessively reducing the doping level to decrease the probability of film cracking can have serious electronic ramifications.

Simulations for non-linear grading profiles produced interesting results. A cathode with a concave-down quadratic profile has a reduced emission barrier, but also is diffusion-limited. A cathode with a concave-up quadratic profile has a large emission barrier, but also has enhanced electron diffusion. As a result, neither non-linear grading profile provided a net increase in current density over the density produced by the linear profile at 300 K. It seems unclear if optimization, by way of a tailored grading profile, could be accomplished.

If these cathodes are simulated in the future, a number of improvements should be considered and implemented. First, in order to obtain more accurate results, the values for the material parameters of the $Al_xGa_{1-x}N$ materials must be more accurately determined. The

key material parameters for cathode operation are electron affinity, donor ionization energy, heterojunction conduction band offset, and electron mobility. Second, there are a number of factors which were left out of the simulations, which deserve further consideration. The possibility of surface states or surface reconstructions were not considered. The effects of having something other than Al, Ga, or N on the emitting surface (e.g., O or C) was not examined. More experimental work is needed to investigate these surface conditions and include them in simulations, if necessary. Third, the Runge-Kutta technique implemented in *Maple V* software on a Sun SPARCstation 4 was adequate for the purposes of this research. However, further simulations of $Al_xGa_{1-x}N$ cathode structures, particularly any attempts involving optimization (through maniupulation of doping, grading, and thickness), may require faster software on a faster computer to keep the computation time reasonable.

It is important to note that as work on $Al_xGa_{1-x}N$ materials continues, $Al_xGa_{1-x}N$ material quality will improve and the material will be much better characterized. Improved growth techniques should result in higher-quality semiconductor material and lead to higher electron mobility. Enhanced electron mobility should ensure that the cathodes are barrier-limited rather than diffusion-limited. Also important is development of the ability to create smooth spatial grading of the Al fraction x.

Acknowledgments

The authors thank R.J. Nemanich (NCSU), R.F. Davis (NCSU), and J.C. Driscoll (PTS Co.) for helpful discussions. This work was financially supported by an ONR STTR grant (Contract No. N00014-97-C-0198) through the PTS Company (Raleigh, NC).

References

[1] S. Strite and H. Morkoc, "GaN, AlN, and InN: A review," *J. Vac. Sci. Technol. B*, vol. 10, pp. 1237-1266, Jul/Aug 1992.

[2] H. Morkoc, S. Strite, G.B. Gao, M.E. Lin, B. Sverdlov, and M. Burns, "Large-band-gap SiC, III-V nitride, and II-VI ZnSe-based semiconductor device technologies," *J. Appl. Phys.*, vol. 76, pp. 1363-1398, Aug. 1, 1994.

[3] P. Kung, A. Saxler, D. Walker, X. Zhang, R. Lavado, K.S. Kim, and M. Razeghi, "$Al_xGa_{1-x}N$ Based Materials and Heterostructures," . *Mat. Res. Soc. Symp. Proc. Vol. 449*, pp. 79-84, 1997.

[4] M.D. Bremser, W.G. Perry, O.H. Nam, D.P. Griffis, R, Loesing, D.A. Ricks, and R.F. Davis, "Acceptor and Donor Doping of $Al_xGa_{1-x}N$ Thin Film Alloys Grown on 6H-SiC(0001) Substrates via Metalorganic Vapor Phase Epitaxy," *Journal of Electronic Materials*, vol. 27, pp. 229-232, 1998.

[5] J. Brown, J. Ramer, K. Zheng, L.F. Lester, S.D. Hersee, and J. Zolper, "Ohmic Contacts to Si-implanted and un-implanted n-type GaN," *Mat. Res. Soc. Symp. Proc. Vol. 395*, pp. 855-860, 1996.

[6] Y.F. Wu, W.N. Jiang, B.P. Keller, S. Keller, D. Kapolnek, S.P. Denbaars, U.K. MIshra, and B. Wilson, "Low resistance ohmic contact to n-GaN with a separate layer method," *Sol. St. Electron.*, vol. 41, pp. 165-168, 1997.
[7] M.C. Benjamin, Cheng Wang, R.F. Davis, and R.J. Nemanich, "Observation of a negative electron affinity for heteroepitaxial AlN on α(6H)-SiC(0001)," *Appl. Phys. Lett.*, vol. 64, pp. 3288-3290, June 13, 1994.
[8] R.J. Nemanich, M.C. Benjamin, S.P. Bozeman, M.D. Bremser, S.W. King, B.L. Ward, R.F. Davis, B. Chen, Z. Zhang, and J. Bernholc, "(Negative) Electron Affinity of AlN and AlGaN Alloys," *Mat. Res. Soc. Symp. Proc. Vol. 395*, pp. 777-788, 1996.
[9] M.C. Benjamin, M.D. Bremser, T.W. Weeks, Jr., S.W. King, R.F. Davis, and R.J. Nemanich, "UV photoemission study of heteroepitaxial AlGaN films grown on 6H-SiC," . *Applied Surface Science*, vol. 104/105, pp. 455-460, 1996.
[10] V.M. Bermudez, T.M. Jung, K. Doverspike, and A.E. Wickenden, "The growth and properties of Al and AlN films on GaN(0001)-(1$\times$1)," *J. Appl. Phys.*, vol. 79, pp. 110-119, Jan. 1, 1996.
[11] C.I. Wu, A. Kahn, E.S. Hellman, and D.N.E. Buchanan, "Electron affinity at aluminum nitride surfaces," *Appl. Phys. Lett.*, vol. 73, pp. 1346-1348, Sept. 7, 1998.
[12] J.L. Shaw, H.F. Gray, K.L. Jensen, and T.M. Jung, "Graded electron affinity electron source," *J. Vac. Sci. Technol. B*, vol. 14, pp. 2072-2079, May/Jun 1996.
[13] J.A. Christman, A.T. Sowers, M.D. Bremser, B.L. Ward, R.F. Davis, and R.J. Nemanich, "Nitride Based Thin Film Cold Cathode Emitters," *Mat. Res. Soc. Symp. Proc. Vol. 449*, pp. 1121-1126, 1997.
[14] A.T. Sowers, J.A. Christman, M.D. Bremser, B.L. Ward, R.F. Davis, and R.J. Nemanich, "Thin films of aluminum nitride and aluminum gallium nitride for cold cathode applications," *Appl. Phys. Lett.*, vol. 71, pp. 2289-2291, Oct. 20, 1997.
[15] C.W. Hatfield and G.L. Bilbro, "Simulation of room temperature thermionic emission from $Al_xGa_{1-x}N$ negative electron affinity cathodes," *J. Vac. Sci. Technol. B*, vol. 17, pp. 552-556, Mar/Apr 1999.
[16] R.F. Davis, personal communication.
[17] J. Singh, *Physics of Semiconductors and Their Heterostructures*, New York: McGraw-Hill, Inc., 1993.
[18] P. Boguslawski and J. Bernholc, "Doping properties of C, Si, and Ge impurities in GaN and AlN," *Physical Review B*, vol. 56, pp. 9496-9504, Oct. 15, 1997.
[19] J.A. Majewski and M. Stadele, "Effects of Substrate Orientation on the Valence Band Splittings and Valence Band Offsets in GaN and AlN Films," *Mat. Res. Soc. Symp. Proc. Vo. 482*, pp. 917-922, 1998.
[20] D.K. Cheng, *Field and Wave Electromagnetics*, New York: Addison-Wesley Publishing Co., 1989.
[21] M.N. Yoder, "Wide Bandgap Semiconductor Materials and Devices," *IEEE Trans. Electron Dev.*, vol. 43, pp. 1633-1636, Oct. 1996.
[22] P.V. O'Neil, *Advanced Engineering Mathematics*, New York: PWS Publishing Co., 1995.
[23] *Maple V*, Waterloo Maple Inc., 450 Phillip St., Waterloo, ON, N2L 5J2, Canada.

[24] S.M. Sze, *Physics of Semiconductor Devices*, New York: John Wiley & Sons, 1981.
[25] M. Sedlacek, *Electron Physics of Vacuum and Gaseous Devices*, New York: John Wiley & Sons, Inc., 1996.